Regular Article

PHYSICAL CHEMISTRY RESEARCH
Published by the
Iranian Chemical Society
www.physchemres.org
info@physchemres.org

***Phys. Chem. Res.**, Vol. 4, No. 1, 1-15, March 2016.*
DOI: 10.22036/pcr.2016.11619

The Nature of Halogen Bonds in $[N\cdots X\cdots N]^+$ Complexes: A Theoretical Study

A. Ebrahimi[a,]*, H. Razmazma and H. Samareh Delarami

Department of Chemistry, Computational Quantum Chemistry Laboratory, University of Sistan and Baluchestan, Zahedan, Iran, P. O. Box: 98135-674

(Received 2 July 2015, Accepted 20 October 2015)

The effects of substituents on the symmetry and the nature of halogen bonds in $[N\cdots X\cdots N]^+$-type systems are presented for the $YC_5H_4N\cdots X\cdots NC_5H_5$ (Y = NO_2, CN, H, CH_3, OCH_3, OH, NH_2, X = Cl, Br, I) complexes. Some structural parameters, energy data and electronic properties were explored with the density functional theory (DFT) calculations. In addition, electrostatic potentials were used in estimation of the strength and the nature of halogen bonds. Results indicate an enhancement effect of the electron-withdrawing substituents on the size of σ-hole and a diminishing effect on the minimum negative electrostatic potential ($V_{S,min}$). A good correlation is observed between the electrostatic potentials and the strengths of two N···X halogen bonds. Furthermore, the results unveiled the effects of the substituents in changing the nature of halogen bonds and indicated that the halogen bonds have a tremendous covalent character in addition to the electrostatic character that usually is considered for the halogen bonds.

Keywords: Halogen-bonding, Bis(pyridine)halonium, σ-Hole, Electrostatic potentials, DFT

INTRODUCTION

Halogen bonding term has been used for non-covalent interactions between halogens and electron donor moieties during the recent decades [1]. Although this interaction has been mainly studied in the gas and solid states, and in silicon [2], few studies have also been devoted to the solution media [3]. Non-covalent intermolecular interactions are important in various fields, such as crystal engineering and material science [4], supramolecular chemistry [5], polymer sciences [6] and biochemistry [7,8]. Halogen bond, which can be depicted as R-X···D, is considered as a relatively powerful oriented non-covalent interaction between the covalently bonded halogen atoms (X) and Lewis bases or other halogen atoms (D) [9,10].

The electronic configuration of valence shell of central halogen $(X)^+$ in $[N\cdots X\cdots N]^+$ complex is s^2p^4, in which the p orbitals are in the $P_x^2P_y^2P_z^0$ form because of induction effects of two Lewis bases. Empty P_Z^0 orbital of the halogen can interact with both electron donor Lewis bases (nitrogens) [11]. The electron-deficient outer lobes of this empty p-orbital of X^+ are called p-holes [12].

It is predicted that the electron-withdrawing power of R can affect the size of σ-hole and X···N bond strength [13]. The halogen bond becomes more powerful with the enhancement of polarization of the halogen atom, as Cl < Br < I [14,15]. Among the halogens, fluorine has the least polarizability and the most electronegativity, and therefore the lowest tendency to form a positive σ-hole and consequently the lowest tendency to form a halogen bond. It can behave as a halogen bond donor in the presence of strong electron withdrawing groups [16]. Recently, Eskandari *et al*. have reported that the interaction of fluorine with Lewis bases cannot be categorized as halogen bond and the F···N interactions should be cited as "fluorine bond" [17].

The lack of electron density in σ-hole forms a positive electrostatic potential area [18]. The strength of the halogen bond is related to the maximum electrostatic potential of positive σ-hole and the anisotropic distribution of charge

*Corresponding author. E-mail: ebrahimi@chem.usb.ac.ir

around the halogen atom [7,19].

Unlike the hydrogen bond, symmetry of the halogen bond is still newfound [21]. Both linear asymmetric and linear symmetric modes are expected for a system with an electropositive atom such as I, Br, Cl and F located between two identical electron donors. The halogen is located at the midway between two electron donors $[N\cdots X\cdots N]^+$ or at a position near to one of the electron donors $[N\text{-}X\cdots N]^+$ [20]. $[N\cdots I\cdots N]^+$ is symmetric in both crystalline structures and solution media, while $[N\cdots Br\cdots N]^+$ is asymmetric in crystalline structures and symmetric in solution media. Different arrangements result in different chemical properties, such as the rate and the efficiency of chemical reactions [10,12].

Although the substituent effects on the halogen bonding [16] and three-center halogen bonds [12,13,16] have been previously studied, this study investigates the substituent effects on the geometry, structure, symmetry and nature of the halogen bonds in the $YC_5H_4N\cdots X\cdots NC_5H_5$ (Y = NO_2, CN, H, CH_3, OCH_3, OH, NH_2; X = Cl, Br, I) complexes, in which an electropositive halonium ion is bonded to two nitrogenous electron donors, by means of quantum chemical calculations, including the quantum theory of atoms in molecules (QTAIM), natural bond orbital (NBO) method, and non-covalent interaction (NCI) index analysis.

COMPUTATIONAL METHODS

All quantum chemical calculations were performed in the gas phase using the Gaussian 09 program package [21]. The structures were fully optimized in a planar geometry by the DFT exchange-correlation functional B97-1 [22]. The cc-pVTZ-PP basis set [23] was used to describe iodine atom and the cc-pVTZ [24] basis set was used to describe other atoms. Rather balanced basis sets were used to check the dependence of results to basis set. Single point calculations have been also performed at B97-1/(H, C, N, O, Cl, Br: cc-pVQZ; I: cc-pVQZ-PP) and B3LYP [25,26]/(I, Br: LANL08d [27] in conjunction with the LANL2DZ effective core potential (ECP) [28-30]; N, Cl: 6-311+G(d,p) [31-33]; O, H, C: 6-311G(d,p) [27,28]) levels of theory. Furthermore, the harmonic vibrational frequency calculations were executed at the same level to ensure that the structures are minima on the potential energy surfaces.

The local topological properties and energy characteristics of the electron charge density at the N-X (X = Cl, Br, I) bond critical points (XBCPs) and the integrated atomic properties on the atomic basins were calculated by the QTAIM method [34] using the AIM2000 [35] software at the MP2 [36]/(Cl, Br, H, C, N, O: aug-cc-pVDZ [19,37]; I: aug-cc-pVDZ-PP [20]) level of theory. In addition, the NBO analysis has been performed on the same level by NBO3.1 program [38]. The electrostatic potentials were calculated with the GaussView5.0 program [39] on the electron density isosurface of 0.001 electrons $Bohr^{-3}$ molecular surface to find the regions that interact with the halogen atoms. The electrostatic potential that is created by the electrons and nuclei of a molecule can be calculated by [40]

$$V(r) = \sum_{\alpha} \frac{Z_\alpha}{|R_\alpha - r|} - \int \frac{\rho(r')}{|r' - r|} dr' \quad (1)$$

in which V(r) is the potential created at any point r by the nuclei and electrons of the molecule; Z_α is the charge on the nucleus α, located at R_α, and ρ(r′) is the electronic density of the molecule and r′ is a dummy integration variable.

Subsequently, the non-covalent interaction regions were calculated at the MP2 [32]/(Cl, Br, H, C, N, O: aug-cc-pVDZ [19,33]; I: aug-cc-pVDZ-PP [20]) level using Multiwfn [41] software and visualized using the VMD program [42].

RESULTS AND DISCUSSION

Molecular Electrostatic Potentials (MEPs)

The MEPs outside the nitrogen atom of the isolated YC_5H_4N were calculated to estimate the potency of that for interaction with the halogen atom (see Fig. 1). Trend in the most negative electrostatic potential ($V_{S,min}$) values is $NO_2C_5H_4N < CNC_5H_4N < C_5H_5N < OHC_5H_4N < CH_3OC_5H_4N < CH_3C_5H_4N < NH_2C_5H_4N$. The electron-donating substituents increase the $V_{S,min}$ value, *i.e.* the N atom becomes a stronger electron donor with the increase of the electron-donating nature of substituent, which enhances the attraction between YC_5H_4N and X^+ (X = Cl, Br, I) ion in the $YC_5H_4N\cdots X^+\cdots NC_5H_5$ (X = Cl, Br, I, Y = NO_2, CN, H, CH_3, OCH_3, OH, NH_2) complexes. The electrostatic

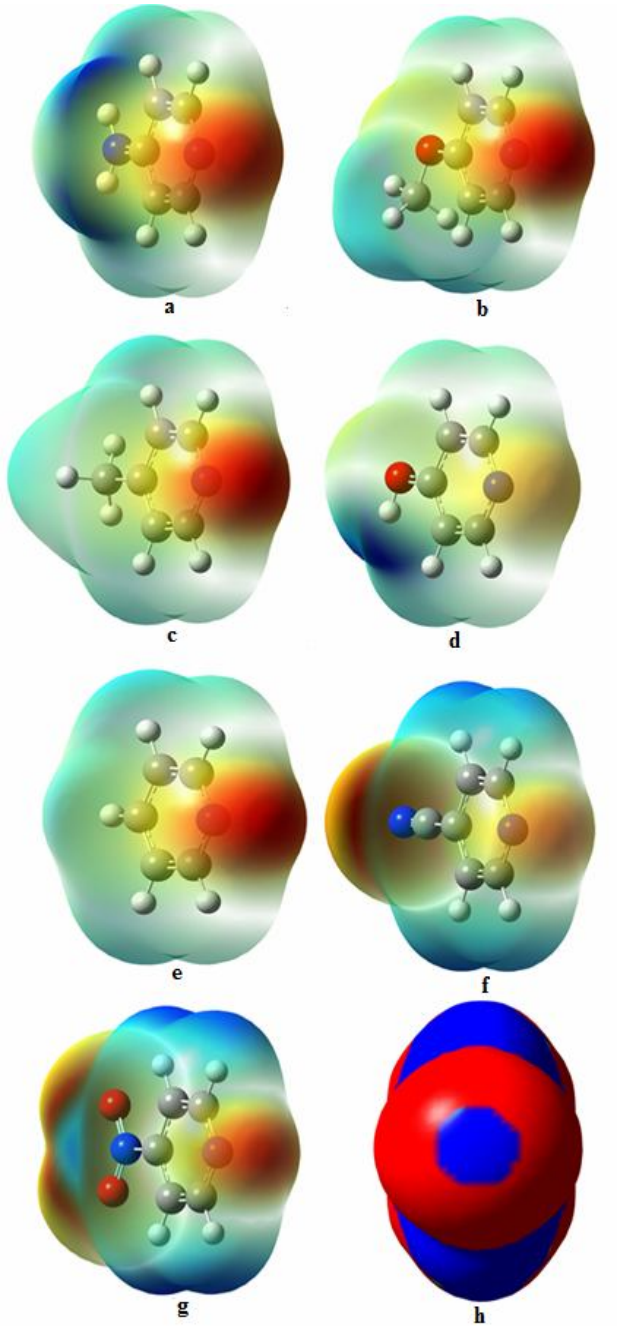

Fig. 1. Electrostatic potentials mapped on the molecular surfaces of $NH_2C_5H_4N$ (a), $CH_3OC_5H_4N$ (b), $CH_3C_5H_4N$ (c), OHC_5H_4N (d), C_5H_5N (e), CNC_5H_4N (f), $NO_2C_5H_4N$ (g), and $C_5H_5NBr^+$ (h) (σ-hole is observed on the halogen units). Color ranges: blue, more positive; green, less positive; yellow, less negative; red, more negative.

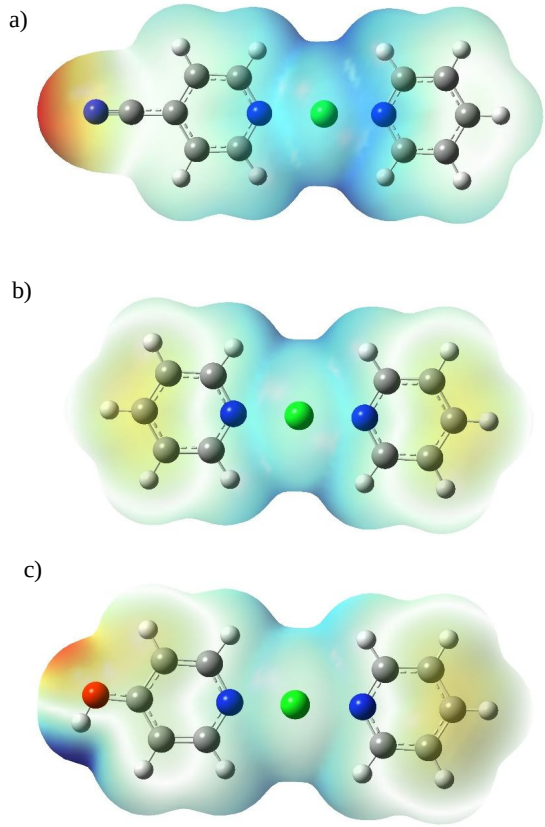

Fig. 2. Electrostatic potentials mapped on the molecular surfaces of $CNC_5H_4N\cdots Cl\cdots NC_5H_5$ (a), $HC_5H_4N\cdots Cl\cdots NC_5H_5$ (b) and $OHC_5H_4N\cdots Cl\cdots NC_5H_5$ (c). The surface was computed on the 0. 08 a.u. contour of the electronic density. Color coding corresponds to - 78.77 kJ mol^{-1} = red < yellow < green < blue = 525.10 kJ mol^{-1}.

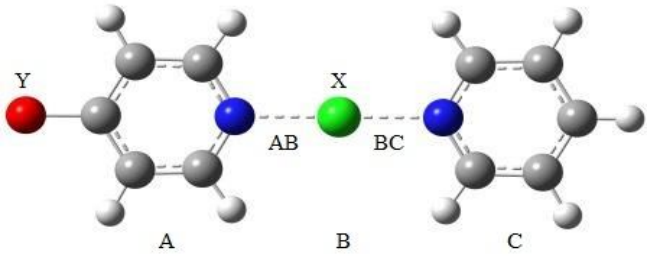

Fig. 3. A typical structure of $YC_5H_4N\cdots X\cdots NC_5H_5$ complexes (Y = NO_2, CN, H, CH_3, OCH_3, OH, NH_2; X = Cl, Br, I).

potential surfaces of the $YC_5H_4N\cdots X^+\cdots NC_5H_5$ complexes have been also presented in Fig. 2, where the positive electrostatic potential region is obvious on the outer surface of the halogen atom. This region is referred as "σ-hole", which is centered on the N-X axis and surrounded by the negative electrostatic potential. Increase in the electron-donation power of substituent is accompanied by decrease in the attraction between unsubstituted C_5H_5N and X^+. For the same substituents Y, the most positive electrostatic potential ($V_{S,max}$) depends on the mass number of the halogen atom and follows I > Br > Cl order. For example, the $V_{S,max}$ value in $CNC_5H_4NCl^+$, $CNC_5H_4NBr^+$ and $CNC_5H_4NI^+$ is equal to 117.6, 128.2 and 143.4 kcal mol^{-1}, respectively. Also, for each halogen atom X, $V_{S,max}$ increases with the increase in the electron-withdrawing power of groups by depletion of electron density on the outer surface of the halogen atom. For example, the $V_{S,max}$ values of $NH_2C_5H_4NBr$, $CH_3OC_5H_4NBr$, $CH_3C_5H_4NBr$, OHC_5H_4NBr, C_5H_5NBr, CNC_5H_4NBr, $NO_2C_5H_4NBr$ are equal to 113.2, 116.4, 118.8, 119.5, 121.8, 128.2 and 129.0 kcal mol^{-1}, respectively. Table 1 lists the $V_{S,max}$ values of halogen atoms and the $V_{S,min}$ values calculated on the nitrogen atoms.

Geometrical Parameters and Vibrational Frequency Analysis

The most important geometrical parameters of planar $YC_5H_4N\cdots X^+\cdots NC_5H_5$ (X = Cl, Br, I, Y = NO_2, CN, H, CH_3, OCH_3, OH, NH_2) complexes, *i.e.* two N···X bond lengths, are given in Fig. 3. All complexes belong to the C_{2V} point group, with the exception of complexes with Y = OH, OCH_3 and CH_3, which belong to the C_S point group. Herein, all systems involve a positively charged halogen located between two nitrogenous electron donors. The N···X···N angle is approximately equal to 180°, so the interactions are highly directional in the complexes.

The geometrical parameters of planar structures are summarized in Table 2. As seen, the intermolecular distances d_{AB} and d_{BC} are in the range of 1.93 to 2.36 Å (see Fig. 3 for d_{AB} and d_{BC} bond lengths). The van der Waals (vdW) radii of the Cl, Br, I and N atoms obtained from X-ray diffraction are equal to 1.75, 1.85, 1.98 and 1.55 Å, respectively [43]. There is an attractive interaction between two subunits, because the X···N distance is significantly shorter than the sum of vdW radii of the X and N atoms in the complexes. The results are in reasonable agreement with the previous results reported by Erdelyi *et al.* [44]. The

Table 1. The Most Positive Electrostatic Potentials ($V_{S,max}$) of σ-Hole Related to the Halogen Atoms in the $YC_5H_4N\cdots X$ Complex and the Most Negative Electrostatic Potentials ($V_{S,min}$) on the Outer Surface of the Nitrogen Atom in the YC_5H_4N Unit in kcal mol^{-1}

X	$V_{S,max}$			$V_{S,min}$
	N···Cl	N···Br	N···I	
H	112.4	121.8	136.3	-36.4
NH_2	104.0	113.2	127.0	-42.2
OH	110.2	119.5	133.6	-37.7
OCH_3	107.2	116.4	130.4	-40.3
CH_3	109.5	118.8	132.9	-38.6
CN	117.6	128.2	143.4	-27.5
NO_2	118.1	129.0	144.4	-27.2

Table 2. The Halogen Bonded Stabilization Energy ΔE, Synergetic Energy E_{syn}, and Individual Interaction Energies E(X···N) in kcal mol^{-1}, and Interaction Distances in Å and Stretching Vibration Frequencies in cm^{-1} for the N···X Bond in the Bis(pyridine)halonium Complexes

	-ΔE			-E(X···N)		d(X···N)		ν(N···X)
	B97-1 [a]	B3LYP	E_{syn}	AB [b]	BC [c]	AB	BC	AB
Cl								
H	**237.76** (237.04)	231.67	150.43	118.88	118.88	1.995	1.995	178.52
NH_2	**246.73** (245.79)	240.15	152.95	177.07	69.66	1.900	2.106	208.44
OH	**240.42** (239.55)	234.24	152.1	136.7	103.72	1.961	2.027	177.58
OCH_3	**242.59** (241.79)	236.42	152.81	154.78	87.8	1.934	2.060	182.87
CH_3	**240.37** (239.66)	234.2	152.25	140.14	100.23	1.959	2.032	181.50
CN	**229.40** (228.70)	223.18	144.57	73.81	155.59	2.083	1.921	207.43
NO_2	**228.67** (227.95)	222.15	142.37	63.27	165.41	2.107	1.904	219.04
Br								
H	**207.07** (206.14)	199.79	115.42	103.54	103.54	2.114	2.114	181.54
NH_2	**215.87** (214.70)	208.11	119.91	130.26	85.61	2.061	2.164	181.73
OH	**209.80** (208.71)	202.45	117.15	111.43	98.37	2.095	2.129	177.45
OCH_3	**211.88** (210.86)	204.53	118.42	119.04	92.84	2.081	2.144	174.41
CH_3	**209.67** (208.74)	202.32	117.35	112.54	97.13	2.095	2.131	178.03
CN	**198.62** (197.70)	191.19	111.59	83.57	115.04	2.153	2.078	187.50
NO_2	**197.82** (196.87)	190.05	110.35	78.68	119.14	2.164	2.069	190.76
I								
H	**172.03** (170.87)	167.85	80.04	86.02	86.02	2.286	2.286	173.54
NH_2	**180.81** (179.42)	176.17	84.26	104.21	76.61	2.244	2.320	171.12
OH	**174.84** (173.53)	170.6	81.57	91.43	83.41	2.271	2.297	169.58
OCH_3	**176.88** (175.63)	172.64	80.95	96.21	80.67	2.261	2.306	168.39
CH_3	**174.63** (173.47)	170.38	81.74	91.64	82.99	2.272	2.297	169.71
CN	**163.66** (162.52)	159.34	76.84	72.6	91.06	2.313	2.262	176.69
NO_2	**162.86** (161.68)	158.2	75.9	69.95	92.91	2.320	2.258	178.64

[a]The bold data correspond to the stabilization energies computed at B97-1/cc-pVTZ level. The data given in the parentheses correspond to the stabilization energies computed at B97-1/cc-pVQZ level. [b]Corresponds to the AB interaction in bis(pyridine)halonium complexes. [c]Corresponds to the BC interaction in bis(pyridine)halonium complexes.

halogen-bond lengths $(X\cdots N)_{AB}$ and $(X\cdots N)_{BC}$ are in very good linear correlations with $V_{S,min}$ and $V_{S,max}$ (see Figs. 4a and 4b).

The vibrational frequencies of the N···X bond in the bis(pyridine)halonium ternary complexes, with a given substituent Y, increase in the order I < Br < Cl (see Table 2). Also, there is a reverse relationship between distance and vibrational frequency for the N···X bond in the complexes with a given halonium ion and different substituents Y, which is in reasonable agreement with the previous findings [45].

Stabilization and Synergetic Energies

The total stabilization energies obtained at three levels of theory are gathered in Table 2. Since similar trends are observed for the halogen-bonded interaction energies obtained at the different levels, the results obtained using the B97-1 method and cc-pVTZ (cc-pVTZ-PP for iodine) basis set are presented in the following discussions.

The individual interaction energies of N···X interactions have been estimated by the exponential relationship between the individual interaction energies (E_{AB} for AB, and E_{BC} for BC pair) and the electron density ρ values calculated at the BCPs (will be discussed in the next section) (Eq. (2)) [45].

$$E_{N\cdots X} = 100a \times (1 - e^{\rho}) \quad (2)$$

The "a" parameter is fitted with converging the Δ (=ΔE - E_{AB} - E_{BC}) value to zero by the Least Square method. ΔE is the total stabilization energy corrected for the BSSE (using the counterpoise method) and the zero-point vibrational energies (Eq. (3)).

$$\Delta E = E_{ABC} - (E_A + E_B + E_C) + BSSE_{ABC} \quad (3)$$

As can be seen in Table 2, the ΔE values of ternary complexes increase in the order I < Br < Cl with a given substituent Y. For example, the ΔE values of $O_2NC_5H_4N\cdots I\cdots NC_5H_5$, $O_2NC_5H_4N\cdots Br\cdots NC_5H_5$ and $O_2NC_5H_4N\cdots Cl\cdots NC_5H_5$ are equal to -162.86, -197.82 and -228.67 kcal mol^{-1}, respectively. For a given halonium ion X^+, the ΔE value decreases with the increase in the electron-withdrawing strength of substituent as NO_2 < CN < H < CH_3 < OH < OCH_3 < NH_2. The E_{AB} and E_{BC} interaction energies correlate with the $V_{S,\ min}$ and $V_{S,\ max}$ values, respectively. The linear correlations are shown in Figs. 4c and 4d. The individual interaction energies estimated by Eq. (2) are given in Table 2. The higher E_{AB} values and the lower E_{BC} values are obtained in the presence of more powerful electron-withdrawing substituents Y.

Table 2 also lists the synergetic energy (E_{syn}), which is an important property in the study of interplay between non-covalent interactions [46], and was calculated using Eq. (4) for ternary complexes [47].

$$E_{syn} = E_{(A\text{-}B\text{-}C)} - E_{(A\text{-}B)} - E_{(B\text{-}C)} \quad (4)$$

where $E_{(A\text{-}B\text{-}C)}$, $E_{(A\text{-}B)}$ and $E_{(B\text{-}C)}$ are stabilization energies of A-B-C, A-B and B-C units, respectively. With the increase in the synergetic energy, the $(N\cdots X)_{AB}/(N\cdots X)_{BC}$ bond length of the $YC_5H_4N\cdots X\cdots NC_5H_5$ (X = Cl, Br, I, Y = NO_2, CN, H, CH_3, OCH_3, OH, NH_2) complexe becomes larger/smaller. These results are in agreement with the equilibrium $d(N\cdots X)_{AB}$ and $d(N\cdots X)_{BC}$ distances. Also, the E_{syn} values increase with the enhancement of electron-withdrawing power of substituents. As seen in Fig. 5, the E_{syn} values are linearly related to the Hammett constants of substituents [48].

AIM Analysis

The electron density ρ calculated at the bond critical point (BCP) is a good criterion to specify the closed-shell interaction (in which ρ is lower than 0.10 au). The corresponding values calculated at the $(X\cdots N)_{AB}$ and $(X\cdots N)_{BC}$ BCPs are presented in Table 3. The ρ_b values calculated at the $(X\cdots N)_{AB}$ and $(X\cdots N)_{BC}$ BCPs are in the range of 0.0656 to 0.1920 and 0.0274 to 0.1296 au, respectively. With a given substituent Y, the trend in the $\rho_{X\cdots N}$ values is Cl > Br > I. The larger ρ_b values are accompanied by the greater interaction energies.

Laplacian of electron density $\nabla^2\rho_{BCP}$, electronic kinetic energy density G_{BCP}, electronic potential energy density V_{BCP}, total energy density H_{BCP}, and $-G_{BCP}/V_{BCP}$ obtained from the AIM analysis at the BCPs, are listed in Table 3. The strength of a chemical bond is generally subdivided in three categories based on the H_{BCP} and $\nabla^2\rho_{BCP}$ values: 1) both $\nabla^2\rho_{BCP}$ and $H_{BCP} > 0$ indicates that "closed-shell"

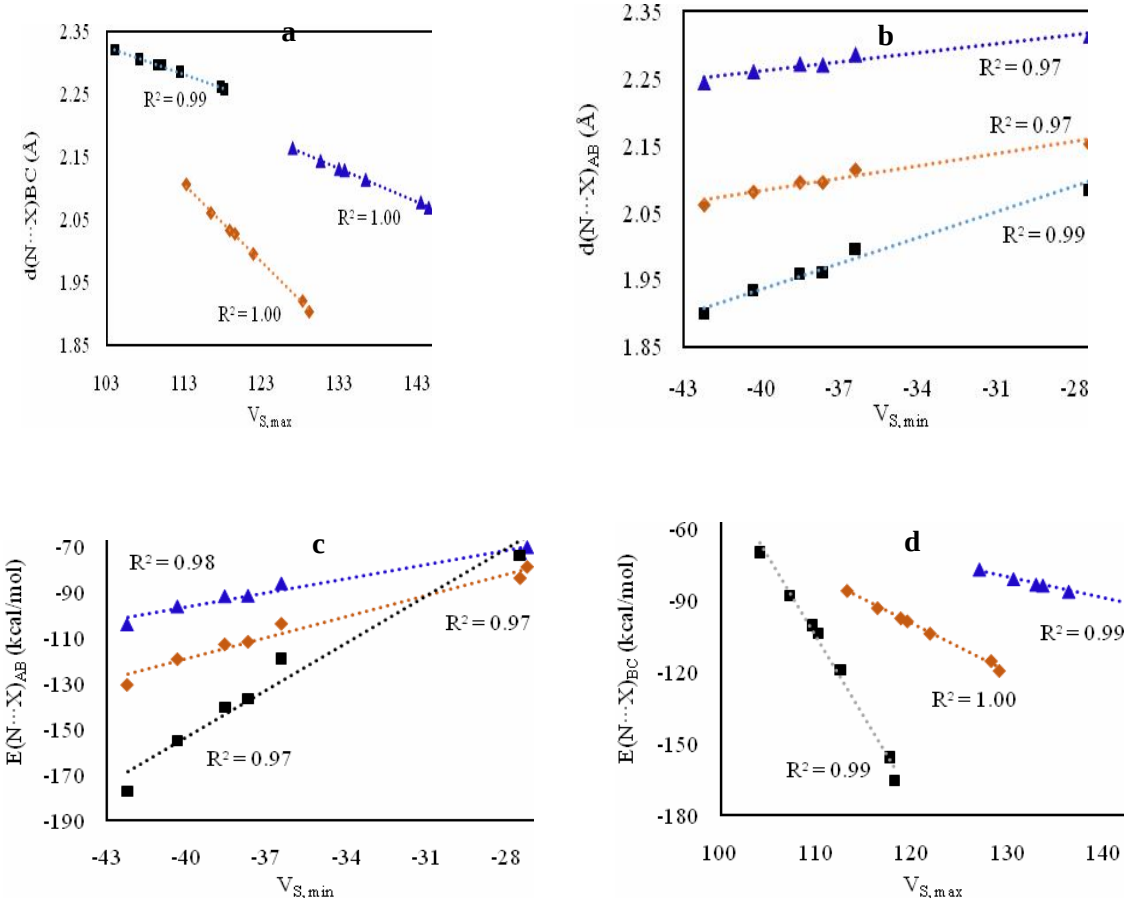

Fig. 4. Linear relationships of the individual halogen-bonded interaction energies E(N···X) and interaction distances d(N···X) with the $V_{S,min}$ and $V_{S,max.}$ R^2 values are given in the parentheses for Cl (■), Br (♦) and I (▲).

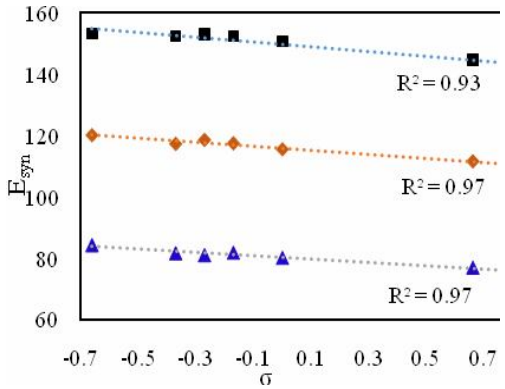

Fig. 5. Linear relationships between the synergetic energy (E_{syn}) and Hammett constants (σ). The values of the Hammett constants of substituents were taken from Ref. [44]. R^2 values are given in the parentheses for Cl (■), Br (♦) and I (▲).

Table 3. The Topological Properties of Electron Charge Density Calculated at the Halogen Bond Critical Points

	$\rho \times 10$	$-\lambda_2 \times 10$	$\nabla^2\rho \times 10$	$G \times 10^2$	$-V \times 10$	$-H \times 10^2$	$-(G/V) \times 10$
Cl							
H	1.057	1.303	1.250	6.72	1.032	3.60	6.514
	1.057	**1.303**	**1.250**	**6.72**	**1.032**	**3.60**	**6.514**
NH_2	1.296	1.654	0.828	8.07	1.408	6.00	5.736
	0.832	**0.959**	**1.416**	**5.41**	**0.729**	**1.87**	**7.429**
OH	1.127	1.404	1.160	7.15	1.140	4.25	6.272
	0.989	**1.198**	**1.318**	**6.32**	**0.934**	**3.02**	**6.765**
OCH_3	1.202	1.517	1.030	7.57	1.256	4.99	6.025
	0.919	**1.091**	**1.373**	**5.91**	**0.838**	**2.47**	**7.048**
CH_3	1.142	1.431	1.137	7.23	1.162	4.39	6.223
	0.974	**1.177**	**1.328**	**6.22**	**0.912**	**2.90**	**6.820**
CN	0.872	1.021	1.401	5.64	0.778	2.14	7.250
	1.242	**1.583**	**0.943**	**7.77**	**1.318**	**5.41**	**5.895**
NO_2	0.821	0.945	1.408	5.32	0.713	1.80	7.469
	1.296	**1.661**	**0.834**	**8.08**	**1.408**	**6.00**	**5.740**
Br							
H	0.903	0.935	1.202	5.84	0.867	2.83	6.732
	0.903	**0.935**	**1.202**	**5.84**	**0.867**	**2.83**	**6.732**
NH_2	0.998	1.049	1.167	6.55	1.019	3.64	6.431
	0.817	**0.825**	**1.231**	**5.28**	**0.748**	**2.20**	**7.057**
OH	0.931	0.967	1.200	6.07	0.914	3.07	6.641
	0.877	**0.902**	**1.213**	**5.68**	**0.832**	**2.64**	**6.822**
OCH_3	0.960	1.003	1.184	6.26	0.957	3.30	6.547
	0.852	**0.870**	**1.222**	**5.51**	**0.797**	**2.46**	**6.918**
CH_3	0.936	0.976	1.194	6.09	0.920	3.11	6.622
	0.873	**0.897**	**1.211**	**5.63**	**0.824**	**2.61**	**6.837**
CN	0.832	0.845	1.231	5.39	0.771	2.31	6.997
	0.970	**1.019**	**1.169**	**6.31**	**0.969**	**3.39**	**6.508**
NO_2	0.811	0.818	1.223	5.23	0.739	2.17	7.068
	0.989	**1.042**	**1.170**	**6.47**	**1.002**	**3.55**	**6.460**
I							
H	0.708	0.599	1.237	4.92	0.674	1.82	7.294
	0.708	**0.599**	**1.237**	**4.92**	**0.674**	**1.82**	**7.294**
NH_2	0.765	0.657	1.329	5.48	0.764	2.16	7.174
	0.659	**0.548**	**1.178**	**4.50**	**0.606**	**1.56**	**7.430**
OH	0.725	0.615	1.272	5.10	0.703	1.92	7.263
	0.694	**0.583**	**1.221**	**4.80**	**0.654**	**1.75**	**7.333**
OCH_3	0.741	0.632	1.290	5.24	0.726	2.02	7.222
	0.680	**0.570**	**1.204**	**4.68**	**0.636**	**1.67**	**7.368**
CH_3	0.726	0.618	1.264	5.09	0.702	1.93	7.250
	0.692	**0.583**	**1.216**	**4.78**	**0.652**	**1.74**	**7.333**
CN	0.667	0.555	1.194	4.58	0.618	1.60	7.417
	0.744	**0.637**	**1.282**	**5.24**	**0.727**	**2.03**	**7.204**
NO_2	0.656	0.543	1.173	4.47	0.601	1.54	7.438
	0.752	**0.646**	**1.301**	**5.33**	**0.741**	**2.08**	**7.194**

The bold values correspond to the BC interaction.

(electrostatic) interactions are dominant, 2) both $\nabla^2\rho_{BCP}$ and $H_{BCP} < 0$ indicates that a "shared-shell" (covalent) interaction is dominant, and 3) $\nabla^2\rho_{BCP} > 0$ and $H_{BCP} < 0$ indicates interaction is partly covalent in the nature [49]. Non-bonded interactions can also be classified on the basis of $-G_{BCP}/V_{BCP}$ ratio. The interaction is shared (covalent) when the ratio is lower than 0.5, is non-covalent when the ratio is higher than 1, and is partly covalent in the nature when the ratio falls between 0.5 and 1 [50]. Table 3 shows that G_{BCP} is smaller than $|V_{BCP}|$, so H_{BCP} value is a small negative number. On the other hand, the $\nabla^2\rho_{BCP}$ values at the X···N BCPs are positive, and $-G_{BCP}/V_{BCP}$ values are between 0.5 and 1 au. This means that the halogen-bonded interactions are partly covalent in these complexes. As reported in Table 3, the values of ρ_{BCP}, $\nabla^2\rho_{BCP}$, and G_{BCP} of $(N\cdots X)_{AB}/(N\cdots X)_{BC}$ become larger/smaller and the values of V_{BCP}, H_{BCP}, and $-G_{BCP}/V_{BCP}$ of $(N\cdots X)_{AB}/(N\cdots X)_{BC}$ become smaller/larger by increasing the electron-withdrawing power of the substituent and the atomic number of halogen. These results indicate that the stronger $(N\cdots X)_{AB}$ bonds with the higher covalent characters are accompanied by the weaker $(N\cdots X)_{BC}$ bonds with lower electrostatic properties. The covalent character of the $(N\cdots X)_{AB}$ interactions is dominate where Y is an electron-donating substituent and the electrostatic character of the $(N\cdots X)_{BC}$ interactions is dominate where Y is a weak electron-withdrawing or an electron-donating substituent.

Figures 6a and 6b present good linear relationships between the $\rho(N\cdots X)_{AB}$ - $V_{S,min}$ and $\rho(N\cdots X)_{BC}$ - $V_{S,max}$ pairs. As can be seen, the higher $V_{S,max}$ values around the X atom are accompanied with the higher ρ_{BCP} values at the $(N\cdots X)_{BC}$ BCPs and stronger XBs. The more negative values of $V_{S,min}$ around the nitrogen atom result in stronger $(N\cdots X)_{AB}$ interactions. Figures 6c and 6d show relationships between the $-G_{BCP}/V_{BCP}$ and the $V_{S,max}$ and $V_{S,min}$ values around the X and N atoms, respectively. The larger $V_{S,max}$ and the lower $V_{S,min}$ values correlate with the lower values of $-G_{BCP}/V_{BCP}$. So, the relationships show that the topological properties such as ρ_{BCP}, G_{BCP} and V_{BCP}, and the electrostatics potential play important roles on the estimation of the nature of these interactions.

In addition to the above mentioned topological properties of electron density, the AIM dual-parameter analysis [50] is also used to evaluate and classify weak to strong interactions using the behavior of H_{BCP} versus $\nabla^2\rho_{BCP}$. In this method, interactions with $\nabla^2\rho_{BCP} > 0$ and $H_{BCP} < 0$ fall in the intermediate region between shared-shell ($\nabla^2\rho_{BCP} < 0$ and $H_{BCP} < 0$) and pure closed-shell interactions ($\nabla^2\rho_{BCP} > 0$ and $H_{BCP} > 0$), where electrons at BCPs are stabilized but not locally concentrated. Herein, the plot of H (N···X) versus $\nabla^2\rho$ (N···X) for both N···X interactions falls in the fourth quadrant (see Fig. 7), and all N···X interactions are proposed to be in the area between shared-shell and pure closed-shell interactions, where the shared-shell nature increases with the electron-withdrawing groups.

Within the framework of the QTAIM, the $L(r) = -1/4\ \nabla^2\rho(r)$ at the (3,+1) CP is particularly interesting to study the nature of XB because its topology shows local charge concentration (CC) and charge depletion (CD) zones as $L(r) > 0$ and $L(r) < 0$, respectively [51,52]. Herein, r is the radial distance from the nucleus to a free spherical atom. The presence of a region of CD at the (3, +1) CP of the L(r) function corresponds to the positive σ-hole in the direction of the halogen bond interaction [53]. This result is in accordance with Politzer's observation about the existence of the σ-hole, a site of CD in the direction of XB interaction, which arises from the decrease of the electronic population along the N···X direction [54].

In the present work, the $\rho(r_{hole})$ values at the (3, +1) CPs of L(r) function were calculated within the range of 0.0278-0.1772, 0.0405-0.0813 and 0.0414-0.0711 au for $YC_5H_4N\cdots Cl\cdots NC_5H_5$, $YC_5H_4N\cdots Br\cdots NC_5H_5$, $YC_5H_4N\cdots I\cdots NC_5H_5$, complexes, respectively. Comparing the $\rho(r_{hole})$ values with the corresponding $V_{S,max}$ values (Table 1) shows that the greater $V_{S,max}$ (or lower $V_{S,min}$) values outside each halogen atom are accompanied by the greater $\rho(r_{hole})$ values.

Non-covalent Interaction (NCI) Index

The NCI index introduced by Yang and co-workers [55-57] provide evidence for the existence of non-covalent interactions, based on the relationship between ρ and the reduced density gradient s [58-60]

$$s \frac{1}{2(3\pi^2)^{\frac{1}{3}}} \frac{|\nabla\rho|}{\rho^{\frac{4}{3}}} \quad (5)$$

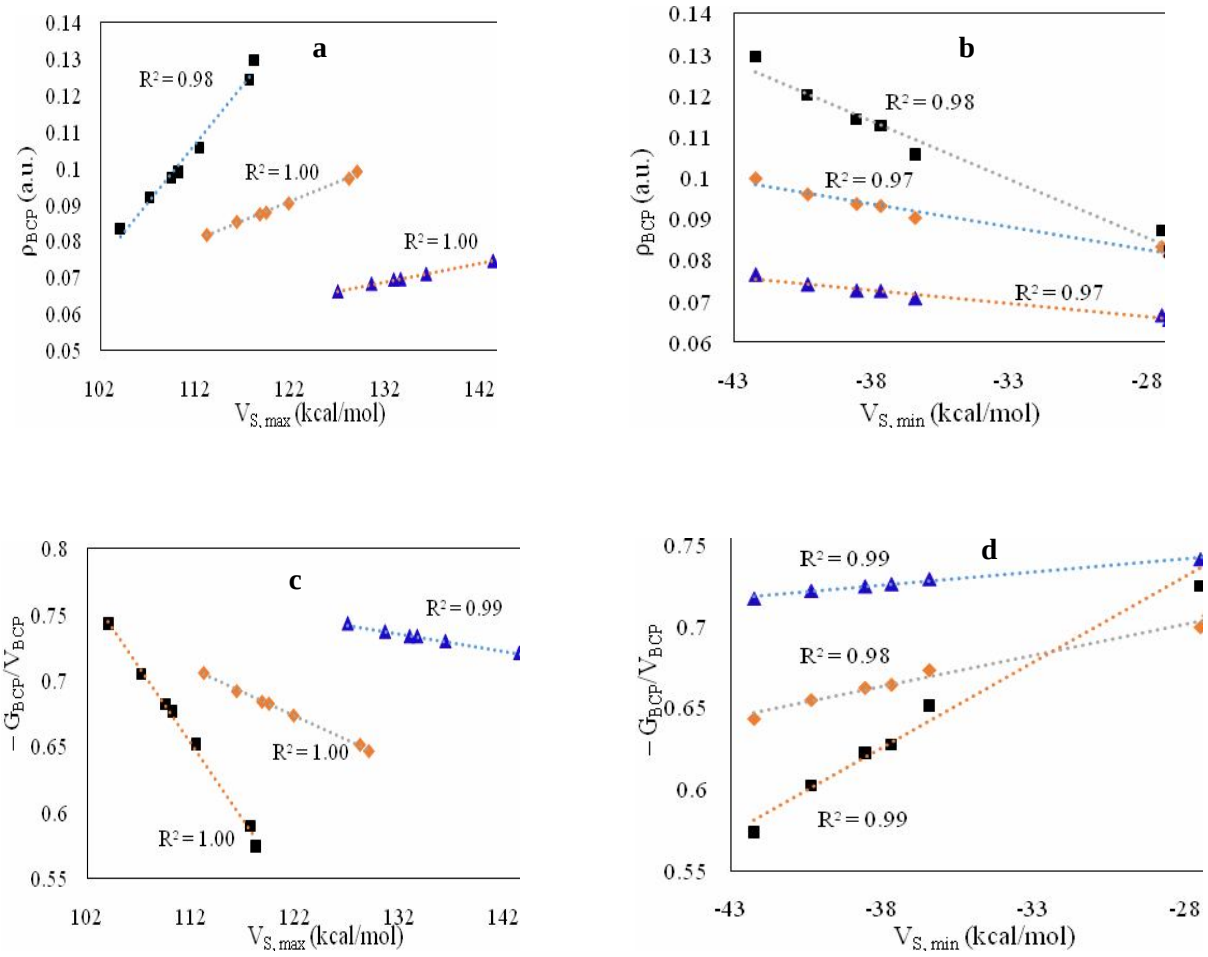

Fig. 6. Linear relationships of ρ_{BCP} and $-G_{BCP}/V_{BCP}$ with the most positive/negative electrostatic potentials $V_{S,min}$ and $V_{S,max}$. R^2 values are given in the parentheses for Cl (■), Br (♦) and I (▲).

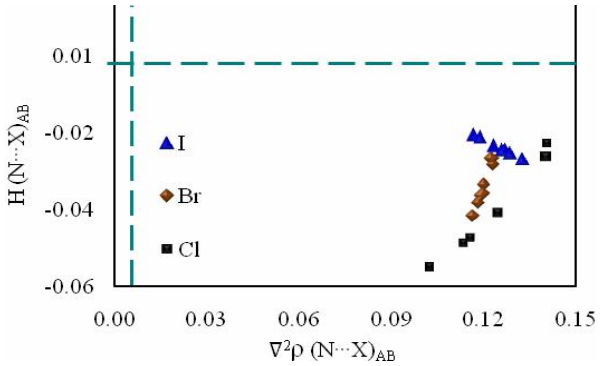

Fig. 7. Plot of H *vs.* $\nabla^2\rho(r)$ at the $(N\cdots X)_{AB}$ BCP.

The NCI analysis is an efficient way to assess the characteristics of the halogen bonds and the location of pairwise atoms connected along the bond path [9]. In QTAIM, the value of ρ is used to estimate the strength of an interaction [61], while the second density Hessian eigenvalue (λ_2) is widely used to investigate different types of non-covalent interactions [30]. According to the definition of Yang and co-workers [55-57], the large value of ρ and $\lambda_2 < 0$ indicate an attractive interaction and the large value of ρ and $\lambda_2 > 0$ implies a nonbonding interaction. Also, a negative λ_2 in NCI region corresponds to a location near to the intermolecular BCP, while a positive λ_2 corresponds to the ring or cage critical point. For example, Fig. 8 shows a graph of the reduced gradient (s) *vs.* sign $(\lambda_2)\rho$ for the $O_2NC_5H_4N\cdots I\cdots NC_5H_5$ and $CH_3OC_5H_4N\cdots I\cdots NC_5H_5$ complexes. On the basis of the scatter plots, low-gradient peaks at low-densities (-0.010 to -0.020 a.u.) indicate the weak non-covalent interactions, which correspond to XB. In the $O_2NC_5H_4N\cdots I\cdots NC_5H_5$ and $CH_3OC_5H_4N\cdots I\cdots NC_5H_5$ complexes, the characteristic peaks directed toward the sign $(\lambda_2)\rho$ values of -0.017 and -0.011, respectively, *i.e.*, the XB interaction in $O_2NC_5H_4N\cdots I\cdots NC_5H_5$ is stronger than $CH_3OC_5H_4N\cdots I\cdots NC_5H_5$ complex. Two principal peaks in Figure 8, where sign $(\lambda_2)\rho > 0.010$, reflect strong steric repulsion and correspond to the non-bonded overlap at the center of rings. Also, Fig. 8 displays the low-gradient isosurface for the $O_2NC_5H_4N\cdots I\cdots NC_5H_5$ and $CH_3OC_5H_4N\cdots I\cdots NC_5H_5$ complexes that agrees with the analysis of the scatter plots.

In the NCI plot, the strength of interaction is identified through color codes: red color indicates strong repulsion, green stands for weak interaction, and blue color signifies a strong attraction such as halogen bonding. The computed NCI regions show that in the midway between the halogen and nitrogen atoms, there is a blue and a red disk isosurface. Electron-withdrawing substituents increase the electrostatic properties and density depletion of $(N\cdots I)_{AB}$ bond relative to $(N\cdots I)_{BC}$ by enhancement of nucleophilicity of the Lewis base (nitrogen atom). Mutually, by reducing the nucleophilicity of the nitrogen atom, electron-donating substituents increase the electrostatic properties and density

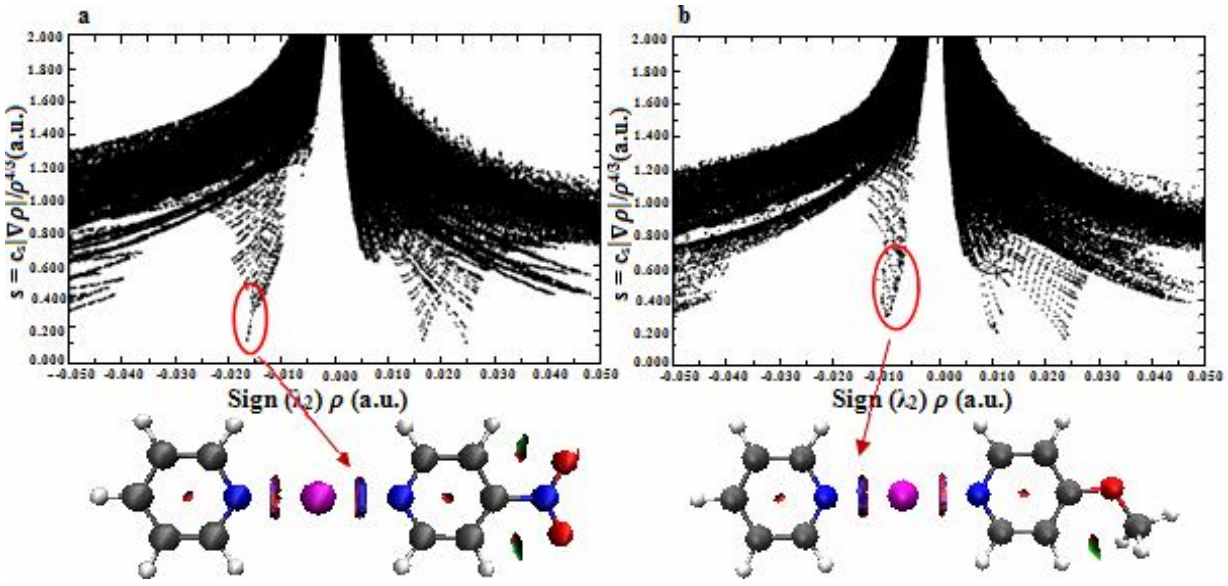

Fig. 8. Plots of the reduced density gradient *vs.* the electron density multiplied by the sign of the second essian eigenvalue (above) and isosurfaces for s = 0.05 a.u. (below) for (a) $O_2NC_5H_4N\cdots X\cdots NC_5H_5$ and (b) $CH_3C_5H_4N\cdots X\cdots NC_5H_5$.

depletion of $(N\cdots I)_{BC}$ bond relative to $(N\cdots I)_{AB}$.

NBO-Based Analysis

Some properties of the halogen bonds can be investigated by the natural bond orbital (NBO) analysis. The data supplied in Table 4 present the most important donor-acceptor orbital interactions and corresponding second-order perturbation stabilization energies $E^{(2)}$ as well as the amount of total charge transfer (CT) from electron donors A and C (see Fig. 3) to the halogen atom. The most important orbital interaction is between the nitrogen lone-pair (LP) orbital and the halogen LP* in the complexes, denoted as LP (N) → LP*(X) (X = Cl, Br, I). The $E^{(2)}$ value shows the tendency of the electron-donor to interact with the electron-acceptor, and will allow us to quantitatively evaluate the charge transfer involved in the formation of the halogen bond.

That orbital interaction, which is affected by substituents, plays an important role on the nature of halogen bonds in the complexes. The LP(A) → LP*(X) orbital interaction is stronger than LP(C) → LP*(X) in the presence of electron-donating substituents, so the electron-donating substituents decrease the electrostatic nature of $(N\cdots X)_{AB}$ bond relative to $(N\cdots X)_{BC}$. The charge transfer gradually increases with the increase of the polarizability of halogen, in agreement with the interaction energies.

The CT value in the $C_5H_5N\cdots Cl\cdots NC_5H_5$, $C_5H_5N\cdots Br\cdots NC_5H_5$ and $C_5H_5N\cdots I\cdots NC_5H_5$ complexes are equal to 0.2849, 0.3932 and 0.5002 (a.u.), so the stronger interaction is accompanied by the higher charge transfer from the electron donor subunit to the halogen atom. As shown in Table 4, the $E^{(2)}$ value of the LP(N) → LP*(X) interaction increases with the increase in the polarizability of halogen from Cl to I in the complexes. Also, the results of NBO analysis indicate that the $E^{(2)}$ value decreases with the increase in the polarizability of the halogen atom.

Table 4. The LP(N) → LP* (X) Donor-Acceptor Interaction Energies $E^{(2)}$ in kcal mol^{-1} and Charge Transfer (CT, e)

	$E^{(2)}$		CT × 10
	AB	BC	(a.u.)
Cl			
H	258.12	258.12	2.849
NH_2	217.28	199.61	2.759
OH	277.89	228.55	2.834
OCH_3	247.83	217.83	2.804
CH_3	273.76	216.92	2.835
CN	195.63	256.29	2.876
NO_2	147.13	404.73	2.935
Br			
H	197.16	197.16	3.932
NH_2	250.28	157.91	3.863
OH	212.15	185.30	3.918
OCH_3	226.39	174.02	3.903
CH_3	214.19	183.01	3.914
CN	163.24	231.33	3.980
NO_2	151.67	244.05	4.000
I			
H	148.62	148.62	5.002
NH_2	178.29	127.87	4.917
OH	157.35	142.56	4.979
OCH_3	164.57	136.97	4.962
CH_3	157.52	141.78	4.978
CN	163.24	231.33	3.980
NO_2	123.16	171.16	5.078

CONCLUSIONS

The results of quantum mechanical calculations on a series of $[N\cdots X\cdots N]^+$-type XBs in the $YC_5H_4N\cdots X\cdots NC_5H_5$ (Y = NO_2, CN, H, CH_3, OCH_3, OH, NH_2, X = Cl, Br, I) ternary complexes can be summarized as follow:

(1) The electron-withdrawing/donating substituents decrease/increase the maximum positive electrostatic potential ($V_{S,max}$) and the minimum negative electrostatic potential ($V_{S,min}$), changing the strength and the nature of halogen bonds in these complexes.

(2) The electron-withdrawing groups of the YC_5H_4N unit enhance the strength of the $(N\cdots X)_{AB}$ bond and increase its covalent nature. Those groups weaken the strength of the $(N\cdots X)_{BC}$ bond and increase its electrostatic nature. The reverse is true for the electron-donating substituents.

(3) Very good linear correlations are observed between

$V_{S,max}$ (or $V_{S,min}$) and the N···X bond length, individual interaction energies E(N···X), topological properties (ρ_{BCP}, $\nabla^2\rho(r)$, G_{BCP}, and V_{BCP}), and Hammet constants σ.

(4) The nature of halogen bonds in the three-center four-electron complexes is determined through inductive and resonance effects of substituents.

REFERENCES

[1] Hassel, O., Structural aspects of interatomic charge-transfer bonding. *Science* **1970**, *170*, 497-502, DOI: 10.1126/science.170.3957.493.

[2] Politzer, P.; Lane, P.; Concha, M. C.; Ma, Y.; Murray, J. S., An overview of halogen bonding. *J. Mol. Model*. **2007**, *13*, 305-311, DOI: 10.1007/ s00894-006-0154-7.

[3] Erdélyi, M., Halogen bonding in solution. *Chem. Soc. Rev*. **2012**, *41*, 3547-3557, DOI:10.1039/c2cs15292d.

[4] Beale, T. M.; Chudzinski, M. G.; Sarwar, M. G.; Taylor, M. S., Halogen bonding in solution: thermodynamics and applications. *Chem. Soc. Rev*. **2013**, *42*, 1667-1680, DOI: 10.1039/c2cs35213c.

[5] 1 Resnati, G.; Metrangolo, P., Halogen Bonding: a paradigm in supramolecular chemistry. *Chem. Eur. J*. **2001**, *7*, 2511–2519, DOI: 10.1002/1521-3765.

[6] Metrangolo, P.; Resnati, G.; Pilati, T.; Liantonio, R.; Meyer, F., Engineering functional materials by halogen bonding. *J. Polym. Sci., Part A; Polym. Chem*. **2007**, *45*, 1-15, DOI: 10.1002/pola.21725.

[7] Auffinger, P.; Hays, F. A.; Westhof, E.; Ho, P. S., Halogen bonds in biological molecules. *Proc. Natl. Acad. Sci. U. S. A*. **2004**, *101*, 16789-16794, DOI: 10.1073/pnas.0407607101.

[8] Poznański, J.; Shugar, D., Halogen bonding at the ATP binding site of protein kinases: preferred geometry and topology of ligand binding. *Biochim. Biophys. Acta* **2013**, *1834*, 1381-9639, DOI: 10.1016/j.bbapap.2013.01.026.

[9] Fourmigué, M., Halogen bonding: recent advances. *Curr. Opin. Solid State Mater. Sci*. **2009**, *13*, 36-45, DOI: 10.1016/j.cossms.2009.05.001.

[10] Metrangolo, P.; Meyer, F.; Pilati, T.; Resnati, G.; Terraneo, G., Halogen bonding in supramolecular chemistry. *Angew. Chem., Int. Ed*. **2008**, *47*, 6114-6127, DOI: 10.1002/anie.200800128.

[11] Carlsson, A. -C. C.; Uhrbom, M.; Karim, A.; Brath, U.; Gräfenstein, J.; Erdélyi, M., Solvent effects on halogen bond symmetry. *Cryst. Eng. Comm*. **2013**, *15*, 3087-3092, DOI: 10.1039/C2CE26745D.

[12] Hakkert, S. B.; Erdélyi, M., Halogen bond symmetry: the N-X-N bond. *J. Phys. Org. Chem*. **2015**, *28*, 226-233, DOI: 10.1002/poc.3325.

[13] Kaur, D.; Kaur, R., Theoretical study on O···Br and O···Cl halogen bonds in some small model molecular systems. *J. Chem. Sci*. **2014**, *126*, 1763-1779, DOI: 10.1007/s12039-014-0717-6.

[14] Politzer, P.; Murray, J. S.; Clark, T., Halogen bonding: an electrostatically-driven highly directional non-covalent interaction. *Phys. Chem. Chem. Phys*. **2010**, *12*, 7748-7757, DOI: 10.1039/c004189k.

[15] Politzer, P.; Murray, J. S., Halogen bonding: an interim discussion. *Chem. Phys. Chem*. **2013**, *14*, 278-294, DOI: 10.1002/cphc.201200799.

[16] Metrangolo, P.; Murray, J. S.; Pilati, T.; Politzer, P.; Resnati, G.; Terraneo, G., The fluorine atom as a halogen bond donor, *viz.* a positive site. *Cryst. Eng. Comm*. **2011**, *13*, 6593-6596, DOI: 10.1039/ c1ce05554b.

[17] Eskandari, K.; Lesani, M., Does fluorine participate in halogen bonding?. *Chem. Eur. J*. **2015**, *21*, 11462-11474, DOI: 10.1002/chem. 2014050 54.

[18] Clark, T.; Hennemann, M.; Murray, J.; Politzer, P., Halogen bonding: the sigma-hole. *J. Mol. Model*. **2007**, *13*, 291-296, DOI: 10.1007/s00894-006-0130-2.

[19] Zordan, F.; Brammer, L.; Sherwood, P., Supramolecular chemistry of halogens: complementary features of inorganic (M-X) and organic (C-X´) halogens applied to M-X···X´-C halogen bond formation. *J. Am. Chem. Soc*. **2005**, *127*, 5979-5989, DOI: 10.1021/ja0435182.

[20] Carlsson, A. -C. C.; Gräfenstein, J.; Budnjo, A.; Laurila, J. L.; Bergquist, J.; Karim, A.; Kleinmaier, R.; Brath, U.; Erdélyi. M., Symmetric halogen bonding is preferred in solution. *J. Am. Chem. Soc*. **2012**, *134*, 5706-5715, DOI: 10.1021/ja301341h.

[21] Frisch, M. J., *et al*. Gaussian 09, Revision A.02, Gaussian, Inc., Wallingford, CT, 2009.

[22] Hamprecht, F. A.; Cohen, A.; Tozer, D. J.; Handy, N. C., Development and assessment of new exchange-correlation functionals. *J. Chem. Phys*. **1998**, *109*, 6264-6271, DOI: 10.1063/1.477267.

[23] Peterson, K. A.; Figgen, D.; Goll, E.; Stoll, H.; Dolg, M., Systematically convergent basis sets with relativistic pseudopotentials. II. Small-core pseudopotentials and correlation consistent basis sets for the post-d group 16-18 elements. *J. Chem. Phys.* **2003**, *119*, 11113-11123, DOI: 10.1063/1.1622924.

[24] Dunning, T. H., Gaussian basis sets for use in correlated molecular calculations. I. The atoms boron through neon and hydrogen. *J. Chem. Phys*. **1989**, *90*, 1007-1023, DOI: 10.1063/1.456153.

[25] Becke, A. D., Density-functional thermochemistry. III. The role of exact exchange. *J. Chem. Phys*. **1993**, *98*, 5648-5652, DOI: 10.1063/1.464913.

[26] Lee, C. T.; Yang, W. T.; Parr, R. G., Development of the colle-salvetti correlation-energy formula into a functional of the electron-density. *Phys. Rev. B: Condens. Matter Mater. Phys.* **1988**, *37*, 785-789, DOI: 10.1103/PhysRevB.37.785.

[27] Roy, L. E.; Hay P. J.; Martin, R. L., Revised basis sets for the LANL effective core potentials. *J. Chem. Theory Comput*. **2008**, *4*, 1029-1031, DOI: 10.1021/ct8000409.

[28] Hay, P. J.; Wadt, W. R., Ab initio effective core potentials for molecular calculations. Potentials for the transition metal atoms Sc to Hg. *J. Chem. Phys.* **1985**, *82*, 270-283, DOI:10.1063/1.448799.

[29] Hay, P. J.; Wadt, W. R., Ab initio effective core potentials for molecular calculations. Potentials for K to Au including the outermost core orbitals. *J. Chem. Phys*. **1985**, *82*, 299-310, DOI:10.1063/1.448975.

[30] Wadt, W. R.; Hay, P. J., Ab initio effective core potentials for molecular calculations. Potentials for main group elements Na to Bi. *J. Chem. Phys*. **1985**, *82*, 284-298, DOI:10.1063/1.448800.

[31] Krishnan, R.; Binkley, J. S.; Seeger R.; Pople, J. A., Selfconsistent molecular orbital methods. XX. A basis set for correlated wave functions. *J. Chem. Phys*. **1980**, *72*, 650-654, DOI:10.1063/1.438955.

[32] Mclean A. D.; Chandler, G. S., Contracted gaussian basis sets for molecular calculations. I. Second row atoms, Z=11-18. *J. Chem. Phys.* **1980**, *72*, 5639-5648, DOI: 10.1063/1.438980.

[33] Clark, T.; Chandrasekhar, J.; Spitznagel, G. W.; Schleyer, P. V., Efficient diffuse function-augmented basis sets for anion calculations. III. The 3-21+G basis set for first-row elements, Li-F. *J. Comput. Chem*. **1983**, *4*, 294-301, DOI: 10.1002/jcc.540040303.

[34] Bader, R. F. W. *Atoms in molecules. A quantum theory*, Oxford University Press, Oxford, 1990; p. 240-279.

[35] Biegler-König, F. *AIM2000*, University of Applied Sciences, Bielefeld, Germany, 2000.

[36] Møller, C.; Plesset, M. S., Note on an approximate treatment for many-electron systems. *Phys. Rev*. **1934**, *46*, 618-622, DOI: 10.1103/Phys.Rev.46.618.

[37] Woon, D. E.; Dunning, T. H., Gaussian basis sets for use in correlated molecular calculations. V. Core-valence basis sets for boron through neon. *J. Chem. Phys*. **1995**, *103*, 4572-4585, DOI: 10.1063/1.470645.

[38] Glendening, E.; Reed, A.; Carpenter, J.; Weinhold, F. Theoretical chemistry institute and department of chemistry; University of Wisconsin: Madison, W.I., 1990.

[39] Frisch, M. J.; Hratchian, H. P.; Dennington, R. D., II; Todd, A.; Keith, T. A.; Millam, J. GaussView 5; Gaussian, Inc., Wallingford, CT, 2009.

[40] Politzer, P.; Truhlar, D. G. Eds.; *Chemical applications of atomic and molecular electrostatic potentials.* Plenum Press: New York, 1981; p 1-6.

[41] Lu, T.; Chen, F., Multiwfn: A multifunctional wavefunction analyzer. *J. Comput. Chem.* **2012**, *33*, 580-592, DOI: 10.1002/jcc.22885.

[42] Humphrey, W.; Dalke, A.; Schulten, K., VMD: visual molecular dynamics. *J. Mol. Graphics Modell*. **1996**, *14*, 33-38, DOI: 10.1016/0263-7855(96)00018-5.

[43] Bondi, A., Van der Waals volumes and radii. *J. Phys. Chem*. **1964**, *68*, 441-451, DOI: 10.1021/j100785a001.

[44] Karim, A.; Reitti, M.; Carlsson, A. -C. C.; Grafenstein J.; Erdelyi, M., The nature of $[N\text{-}Cl\text{-}N]^+$ and $[N\text{-}F\text{-}N]^+$ halogen bonds in solution. *Chem. Sci*.

2014, *5*, 3226-3233, DOI: 10.1039/c 4 sc01175a.

[45] Ebrahimi, A.; Habibi Khorassani, S. M.; Delarami, H., Estimation of individual binding energies in some dimers involving multiple hydrogen bonds using topological properties of electron charge density. *Chem. Phys*. **2009**, *365*, 18-23, DOI:10.1016/ j.chemphys.2009.09.013.

[46] Lu, Y.; Liu, Y.; Li, H.; Zhu, X.; Liu, H.; Zhu, W., Mutual influence between halogen bonds and cation-π interactions: a theoretical study. *Chem. Phys. Chem*. **2012**, *13*, 2154-2161, DOI: 10.1002/ cphc.201200035.

[47] Lucas, X.; Estarellas, C.; Escudero, D.; Frontera, A.; Quiñonero, D.; Dey, P. M., Very long-range effects: cooperativity between anion-π and hydrogen-bonding interactions. *Chem. Phys. Chem*. **2009**, *10*, 2256-2264, DOI: 10.1002/cphc.200900157.

[48] Alkorta, I.; Sánchez-Sanz, G.; Elguero, J., Linear free energy relationships in halogen bonds. *Cryst. Eng. Comm*. **2013**, *15*, 3178-3186, DOI: 10.1039/ C2CE26739J.

[49] Rozas, I.; Alkorta, I.; Elguero, J., Behavior of ylides containing N, O, and C atoms as hydrogen bond acceptors. *J. Am. Chem. Soc*. **2000**, *122*, 11154-11161, DOI: 10.1021/ja0017864.

[50] Nakanishi, W.; Hayashi, S.; Narahara, K., Atoms-in-molecules dual parameter analysis of weak to strong interactions: behaviors of electronic energy densities versus Laplacian of electron densities at bond critical points. *J. Phys. Chem. A*. **2008**, *112*, 13593-13599, DOI: 10.1021/jp8054763.

[51] Popelier, P., On the full topology of the Laplacian of the electron density. *Coord. Chem. Rev*. **2000**, *197*, 169-189, DOI: 10.1016/S0010-8545(99)00189-7.

[52] Madzhidov, T. I.; Chmutova, G. A., The nature of the interaction of dimethyl selenide with IIIA group element compounds. *J. Phys. Chem. A*. **2013**, *117*, 4011-4024, DOI: 10.1021/jp312383f.

[53] Duarte, D. J.; Sosa, G. L.; Peruchena, N. M., Nature of halogen bonding. A study based on the topological analysis of the Laplacian of the electron charge density and an energy decomposition analysis. *J. Mol. Model*. **2013**, *19*, 2035-2041, DOI: 10.1007/ s00894-012-1624-8.

[54] Duarte, D. J.; Margarita, M.; Peruchena, N. M., Topological analysis of aromatic halogen/hydrogen bonds by electron charge density and electrostatic potentials. *J. Mol. Model*. **2010**, *16*, 737-748, DOI: 10.1007/s00894-009-0558-2.

[55] Contreras-Garcia, J.; Johnson, E. R.; Keinan, S.; Chaudret, R.; Piquemal, J-P.; Beratan, D. N.; Yang, W., NCIPLOT: a program for plotting noncovalent interaction regions. *J. Chem. Theory Comput*. **2011**, *7*, 625-632, DOI: 10.1021/ct100641a.

[56] Contreras-García, J.; Yang, W.; Johnson, E. R., Analysis of hydrogen-bond interaction potentials from the electron density: integration of noncovalent interaction regions. *J. Phys. Chem. A*. **2011**, *115*, 12983-12990, DOI: 10.1021/jp204278k.

[57] Johnson, E. R.; Keinan, S.; Mori-Sanchez, P.; Contreras-Garcia, J.; Cohen, A. J.; Yang, W., Revealing noncovalent interactions. *J. Am. Chem. Soc*. **2010**, *132*, 6498-6506, DOI: 10.1021/ ja100936w.

[58] Hohenberg, P.; Kohn, W., Inhomogeneous electron gas. *Phys. Rev*. **1964**, *136*, B864-871.

[59] Cohen, A. J.; Mori-Sánchez, P.; Yang, W., Insights into current limitations of density functional theory. *Science* **2008**, *321*, 792-794, DOI: 10.1126/science. 1158722.

[60] Becke, A. D. Modern electronic structure theory; world scientific: River Edge, *NJ*. **1995**, 1022-1046.

[61] Xu, L.; Sang, P.; Zou, J.-W.; Xu, M.-B.; Li, X.-M.; Yu, Q.-S., Evaluation of nucleotide C-Br···O-P contacts from ONIOM calculations: theoretical insight into halogen bonding in nucleic acids. *Chem. Phys. Lett*. **2011**, *509*, 175-180, DOI:10.1016/ j.cplett.2011.04.102.